NPL Report CEM 13

Correction model for nonuniform gap distributions in parallel-plate dielectric resonator measurements

L R Arnaut

Center for Electromagnetic Metrology
National Physical Laboratory
Queens Road
Teddington
Middlesex TW11 0LW
United Kingdom

May 1999

Abstract

Correction formulas are derived for nonuniform gaps in a parallel-plate dielectric resonator configuration. This correction model enables the accuracy of the characterization of dielectric resonators to be improved. The model accounts for uncertainties due to complex gap profiles that may exist between the sample and the upper and lower resonator plates as a result of machining. The analysis is based on a polynomial expansion of the functions which characterize the profiles of the interfaces of the dielectric specimen and the resonator plates. It allows for gap profiles of algebraic but otherwise arbitrary complexity. The replacement of geometrically averaged gap widths by electromagnetically weighted average gap widths is found to yield a marked effect, in particular, for the $TE_{01\delta}$ mode. Numerical examples are given for the case of linear and parabolic gap profiles.

Keywords: dielectric resonators, low-loss dielectrics, parallel-plate measurements, Hakki–Coleman method, Courtney holder, nonuniform gaps, weighted gap correction, polynomial expansion.

ISSN 1369-6742

National Physical Laboratory
Teddington, Middlesex TW11 0LW, United Kingdom

Approved on behalf of the Managing Director of NPL by
Dr S Pollitt, Head of the Center for Electromagnetic Metrology

Contents

List of Tables

List of Figures

1 Introduction

The cylindrical parallel-plate dielectric resonator measurement technique, also known as the Hakki–Coleman method or Courtney holder, is a widely used technique for measuring dielectric properties of low-loss, high-permittivity specimens that is simple and yet capable of achieving high accuracies [7, 8]. In search for further increasing the measurement accuracy, one of the main sources of measurement uncertainty is the occurrence of gaps[1] uniform or not, which exist between the specimen interfaces and the resonator plates. Such gaps may be due to imperfections as a result of machining of specimen and plates. Alternatively, such gaps may have been introduced deliberately to avoid direct abrasive contact between plates and specimen or to achieve higher quality factors, by using a low-permittivity spacer. These gaps become especially important in the measurement of short, very high permittivity dielectric resonators, where they have a significant effect on the measured resonance characteristics, i.e. the resonance frequency f_{res} and unloaded quality factor Q. Uniform, i.e. constant-width gaps can be corrected for using simplified models [1, 2] or rigorous techniques for axially symmetric configurations [4, 5, 6]. Full-wave numerical analyses are generally required for more complex distributions of the gap profile, particularly those that do not exhibit azimuthal symmetry. However, the very fine mesh required in such simulations, locally or globally, together with numerical artefacts (e.g. errors due 'staircasing' when modelling complex boundaries, computation time, stability, ...) limit their accuracy and feasibility.

In this paper we propose a gap correction model using polynomial expansion of a complex gap profile. Due to the nature of machining of resonator plates and specimens, interfaces with azimuthal symmetry but algebraically varying radial distributions form an fundamental and important class of gap profile distributions. Explicit expressions for effective gap widths for such distributions are presented below. Still more general radial gap profiles that are due to rough or grooved surfaces can be accounted for with the present technique by expressing these in terms of the canonical profiles. Because of the azimuthal symmetry, such gaps could be analyzed rigorously using radial [4] or axial [6] mode matching. However, this is computationally more demanding than the simpler techniques, especially because the top and bottom interfaces are no longer perpendicular to the cylindrical axis so that the integrations involved must be performed numerically. The technique presented in this paper can be used in conjunction with the simpler analysis models for parallel-plate dielectric resonators (e.g. Itoh–Rudokas technique [2, 7]) in order to increase their accuracy for realistic gap distributions.

[1] The term *gaps* is used here as a collective term for any space that has a permittivity different from that of either the specimen or the conducting plates. Hence the notion is not restricted to air gaps, but also comprises dielectric spacer material.

2 Gap modelling

For the canonical nonuniform gaps, the height z of each one of the two interfaces j forming gap i is taken to be an algebraic function of the radial distance r from the axis of the specimen:

$$z_{ij}(r) = z_{ij}(0) + a_{ij}\, r^{\alpha_{ij}} \qquad (i = 0, 1, \ldots;\ j = 0, 1) \tag{1}$$

Integer values 0, 1, 2, 3, ... for α_{ij} correspond to parallel and linearly, parabolically, cubically, ... tapered interfaces as special cases, respectively. The heights along the axis, $z_{ij}(0)$, are taken as nominal values for the gap width. More general nonuniform gaps can be modelled using polynomial expansion to order N_{ij}:

$$z_{ij}(r) = \sum_{k=0}^{N_{ij}} a_{ijk}\, r^{\alpha_{ijk}} \tag{2}$$

The coefficients a_{ijk} can be obtained by performing N_{ij} gauge measurements of the specimen and plates, relative to a reference plane, along one radius. If a reference plane is not available to characterize the interface profiles $z_{ij}(r)$ individually, then the expansion coefficients can be obtained to first approximation from specimen thickness measurements by assuming that the radial profiles are identical at both ends, viz. $z_{01} = z_{10}$. For the special case of $N_{ij} = 0$, the values a_{ij0} correspond to $\alpha_{ij0} = 0$ and give rise to a 0th-order uniform gap approximation.

Nonuniform gap widths give rise to a twofold nonuniformity. The first kind of nonuniformity is due to the variation of the gap width across the interface, assuming that the transverse field is radially uniform across the interfaces. This is the 'geometrical' nonuniformity, for which the complex gap prfile can be replaced by an effective gap width being the integrated gap profile across the transverse cross-section. However, the actual nonuniformity of the transverse field weighs local gap width according to the local field strength. This yields a second, i.e. 'electromagnetic' nonuniformity. Only if the gap or the transverse fiel strength are both types uniform degenerate. For a complex gap profile, the electromagnetic nonuniformity must be used. More specifically, effective uniform gap widths Δ_i can be defined as averages on either end of the specimen weighted by the local electromagnetic field strength. For general HEM_{mnp} modes:

$$\Delta_i = \frac{\int_0^a w_m(k_{\rho 1} r)\,[z_{i1}(r) - z_{i0}(r)]\, r\mathrm{d}r}{\int_0^a w_m(k_{\rho 1} r)\, r\mathrm{d}r} \tag{3}$$

where $w_m(k_{\rho 1} r)$ are radial weighting coefficients which originate from the corresponding radial dependence of transverse electric and magnetic fields components [7]. For integer values of α_{ijk}

the integrals can be solved explicitely with the aid of the following relations between Bessel functions:

$$\int x^{\alpha} J_m(x)\mathrm{d}x = -x^{\alpha} J_{m-1}(x) + (\alpha + m - 1)\int x^{\alpha-1} J_{m-1}(x)\mathrm{d}x \tag{4}$$

$$\int x^{\alpha} J_0(x)\mathrm{d}x = x^{\alpha} J_1(x) + (\alpha - 1)x^{\alpha-1} J_0(x) - (\alpha - 1)^2 \int x^{\alpha-2} J_0(x)\mathrm{d}x \tag{5}$$

$$\int x^2 J_0(x)\mathrm{d}x = x^2 J_1(x) + x J_0(x) - \int J_0(x)\mathrm{d}x \tag{6}$$

$$\int x J_0(x)\mathrm{d}x = x J_1(x) \tag{7}$$

$$\int J_1(x)\mathrm{d}x = -J_0(x) \tag{8}$$

For ready reference, Tbls 1–4 list expressions for Δ_i for the thus obtained first few values of α and m for the practically important TE_{mnp} modes. For larger m or for other modes, numerical computation is advisable. The coefficients A_m and B_m are different for the ϕ- and ρ-components of the field, and are given as A_m^{ϕ}, B_m^{ϕ} and A_m^{ρ}, B_m^{ρ} as listed in Tbl 5. The amplitude coefficients A_m and B_m are specified to an arbitrary constant factor, but have a fixed ratio [7]:

$$C_m \triangleq \frac{B_m}{A_m} = \frac{k_0}{m\beta}\left[\epsilon_r{}^{\frac{1}{2}} \frac{x^{-1}}{x^{-2}+y^{-2}} \frac{J_m'(x)}{J_m(x)} + \epsilon_r{}^{-\frac{1}{2}} \frac{y^{-1}}{x^{-2}+y^{-2}} \frac{K_m'(y)}{K_m(y)}\right] \tag{9}$$

hence all gaps are completely specified.

3 Numerical example

We shall further concentrate on a single gap profile $\Delta_0 \triangleq \Delta$, between a perfectly flat surface and a single interface ($j = 0$) described by coefficients $a_{00k} \triangleq a_k$. Figs 1 and 2 show Δ/L for general values of linear and parabolic gap profiles for a lossless ceramic specimen of radius $a = 15.000$mm, axial specimen length $L = 12.030$mm and relative permittivity $\epsilon_r = 36.41$. The local gap widths are assumed to increase monotonously with radial distance, in accordance with the specific profile, from zero value at the axis of the specimen. In each one of the two simulations, the local gap width as an extension of the side surface of the specimen at $r = a$ ranges from 1μm to 3mm in half decade steps.

For an assumed linear gap profile, it thus follows that the gap nonuniformity results in a correction of -0.75%, 99.8%, 18.6% and 12.6%, relative to the geometrical average gap width, for the TE_{0np}, TE_{1np},TE_{2np} and TE_{3np} mode, respectively. For the parabolic gap profile, the contribution of the gap nonuniformity increases in magnitude to -3.5%, 160%, 30.7% and 19.1% for the respective modes.

4 Inversion

The effective, i.e. electromagnetically homogenized, gaps Δ_i are implicit functions of ϵ through the radial wavenumber k_ρ. The value of k_ρ is obtained by solving the transcendental eigenvalue equation for the particular mode of interest. If the dielectric properties of the material are unknown then these can be obtained through inversion as follows. First, 0th-order approximations $\Delta_i^{(0)} \triangleq \langle |z_{i1} - z_{i2}| \rangle$ for the homogenized gap widths are computed using nonweighted averaging across the transverse cross-section of the dielectric specimen. These are obtained by replacing the Bessel functions in Eqn (3) by unity, i.e. assuming a uniform distribution for the transverse field. These gap approximations $\Delta_i^{(0)}$ are subsequently used together with the measured resonance characteristics f_{res} and Q_u for the mode in question to yield 1st-order approximations for ϵ and $\tan\delta$ which correspond to actual transverse fields. This can be done, for example, using a simple Itoh–Rudokas model [2] in an iterative loop or using other methods [3], possibly augmented by a variational correction. The obtained 1st-order estimate $\epsilon^{(0)}$ is then used to subsequently compute an improved value of $k_{\rho 1}$. This is finally used to update the value of $\Delta_i^{(0)}$ to $\Delta_i^{(1)}$ from Eqn (3). The iteration can be repeated until a specified tolerance on ϵ or $\tan\delta$ has been reached.

A rigorous axial or radial mode matching technique for analysis is hampered by the fact that the solution to the wave equation cannot be separated into radial and axial eigenfunctions for the configuration of interest. We approximate the solution by considering a weighted uniform 'gap' of constant height Δ and a weighted uniform effective permittivity $\epsilon_{eff,i}$:

$$\epsilon_{eff,i} = \frac{\int_0^a r\mathrm{d}r \int_{z_{ij}(0)}^{z_{ij}(a)} J_n(k_{\rho 1} r)\epsilon(r,z)\mathrm{d}z}{\int_0^a r\mathrm{d}r \int_{z_{ij}(0)}^{z_{ij}(a)} J_n(k_{\rho 1} r)\mathrm{d}z} \tag{10}$$

5 Conclusions

The electromagnetic weighting of complex gap profiles is found to yield a correction to geometric averaging of the gap width. The magnitude of this correction ranges over several orders of magnitude, depending on the mode in question. Because the correction for the $\mathrm{TE}_{01\delta}$ is generally small (order of a few percent), the effect on the inversion procedure to calculate the complex permittivity is equally small. However, accurate inversion procedures not only consider the $\mathrm{TE}_{01\delta}$ mode, but also more (if possible, all) measurable and identifiable resonant modes, for which the corrections appear to be significantly larger. Thus, each mode should be attributed a different, mode-dependent gap width to improve on the accuracy of the characterization of the specimen.

6 Acknowledgement

This work was sponsored by EC Project SMT4–CT96–2118 'Electrotechnical Characteristics of Advanced Technical Ceramics and Their Measurement' and through the UK Department of Trade and Industry National Measurement System Electrical Programme.

References

[1] Cohn, S B: Microwave bandpass filters containing high-Q dielectric resonators; *IEEE Trans MTT,* vol 16 (1968), pp 218–227.

[2] Itoh, T; Rudokas, R S: New method for computing the resonance frequencies of dielectric resonators; *IEEE Trans MTT,* vol 25 no 1 (1977), pp 52–54.

[3] Guillon, P; Garault, Y: Accurate resonant frequencies of dielectric resonators; *IEEE Trans MTT,* vol 25 no 11 (1977), pp 916–922.

[4] Kobayashi, Y; Fukuoka, N; Yoshida, S: Resonant modes for a shielded dielectric resonator; *IEICE Trans Electron,* vol E64-B no 11 (1981), pp 44–51.

[5] Crombach, U; Michelfeit, R: Resonanzfrequenzen und Feldstarken in geschirmten Scheiben- und Ringresonatoren; *Frequenz,* vol 25 no 12 (1981), pp 324–328.

[6] Hong, U S; Jansen, R H: Veränderung der Resonanzfrequenzen dielektrischer Resonatoren in Mikrostripschaltungen durch Umgebungsparameter; *Archiv Elekr Übertr,* vol 38 no 2 (1984), pp 106–112.

[7] Kajfez, D and Guillon, P: *Dielectric Resonators*; Vector Fields, Oxford, MI (1990), Secs. 4.4–4.5.

[8] Kobayashi, Y; Tamura, H: Round robin test on a dielectric resonator method for measuring complex permittivity at microwave frequency; *IEICE Trans Electron,* vol E77-C no 6 (1994), pp 882–887.

7 Tables

$m = 0$	
α	Δ
0	a_0
1	$\frac{a_1}{k_\rho}\frac{x^2J_0(x)-2xJ_1(x)}{xJ_0(x)-X_0}$
2	$\frac{a_2}{k_\rho^2}\frac{x^3J_0(x)-3x^2J_1(x)-3xJ_0(x)+3X_0}{xJ_0(x)-X_0}$

Table 1: Expressions for effective gap width for first few values of order α and radial mode number $m = 0$, with $x \triangleq k_\rho a$, $X_0(x) \triangleq \int_0^x J_0(y)dy$ and $X_0(x) \to 1$ for $x \to \infty$.

$m = 1$	
α	Δ
0	a_0
1	$\frac{a_1}{k_\rho}\frac{A_1x^2J_1(x)+(4A_1-B_1)[xJ_0(x)-X_0]}{2A_1xJ_1(x)+(2A_1-B_1)[J_0(x)-1]}$
2	$\frac{a_2}{k_\rho^2}\frac{2A_1x^3J_1(x)+(6A_1-B_1)x^2J_0(x)+(-12A_1+2B_1)xJ_1(x)}{2A_1xJ_1(x)+(2A_1-B_1)[J_0(x)-1]}$

Table 2: Expressions for effective gap width for first few values of order α and radial mode number $m = 1$, with $x \triangleq k_\rho a$, $X_0(x) \triangleq \int_0^x J_0(y)dy$ and $X_0(x) \to 1$ for $x \to \infty$.

$m = 2$	
α	Δ
0	a_0
1	$\frac{a_1}{k_\rho}\frac{A_2x^2[J_2(x)-J_0(x)]+(6A_2-B_2)xJ_1(x)+(8A_2-2B_2)[J_0(x)-1]}{A_2x[J_2(x)-J_0(x)]+(6A_2-2B_2)J_1(x)+(-2A_2+B_2)X_0}$
2	$\frac{a_2}{k_\rho^2}\frac{A_2x^3[J_2(x)-J_0(x)]+(8A_2-B_2)x^2J_1(x)+(18A_2-3B_2)xJ_0(x)+(-18A_2+3B_2)X_0}{A_2x[J_2(x)-J_0(x)]+(6A_2-2B_2)J_1(x)+(-2A_2+B_2)X_0(x)}$

Table 3: Expressions for effective gap width for first few values of order α and radial mode number $m = 2$, with $x \triangleq k_\rho a$, $X_0(x) \triangleq \int_0^x J_0(y)\mathrm{d}y$ and $X_0(x) \to 1$ for $x \to \infty$.

$m = 3$	
α	Δ
0	a_0
1	$\frac{a_1}{k_\rho}\frac{A_3x^2[J_3(x)-J_1(x)]+(5A_3-B_3)xJ_2(x)-3A_3xJ_0(x)+(30A_3-6B_3)J_1(x)+(-12A_3+3B_3)X_0(x)}{A_3x[J_3(x)-J_1(x)]+(4A_3-B_3)J_2(x)-2A_3[J_0(x)-1]+(8A_3-2B_3)[J_1(x)/x-1/2]}$
2	$\frac{a_2}{k_\rho^2}\frac{A_3x^3[J_3(x)-J_1(x)]+(6A_3-B_3)x^2J_2(x)-4A_3x^2J_0(x)+(32A_3-4B_3)xJ_1(x)+(48A_3-8B_3)[J_0(x)-1]}{A_3x[J_3(x)-J_1(x)]+(4A_3-B_3)J_2(x)-2A_3[J_0(x)-1]+(8A_3-2B_3)[J_1(x)/x-1/2]}$

Table 4: Expressions for effective gap width for first few values of order α and radial mode number $m = 3$, with $x \triangleq k_\rho a$, $X_0(x) \triangleq \int_0^x J_0(y)\mathrm{d}y$ and $X_0(x) \to 1$ for $x \to \infty$.

m	A_m^ϕ	B_m^ϕ	A_m^ρ	B_m^ρ
1	$j\frac{\omega\mu_o}{2}C_1$	$j\beta$	$-j\frac{\beta}{2}$	$-j\omega\mu_o C_1$
2	$j\frac{\omega\mu_o}{2}C_2$	$j2\beta$	$-j\frac{\beta}{2}$	$-j2\omega\mu_o C_2$
3	$j\frac{\omega\mu_o}{2}C_3$	$j3\beta$	$-j\frac{\beta}{2}$	$-j3\omega\mu_o C_3$

Table 5: Coefficients A_m and B_m for use with Tables 1–4.

8 Figures

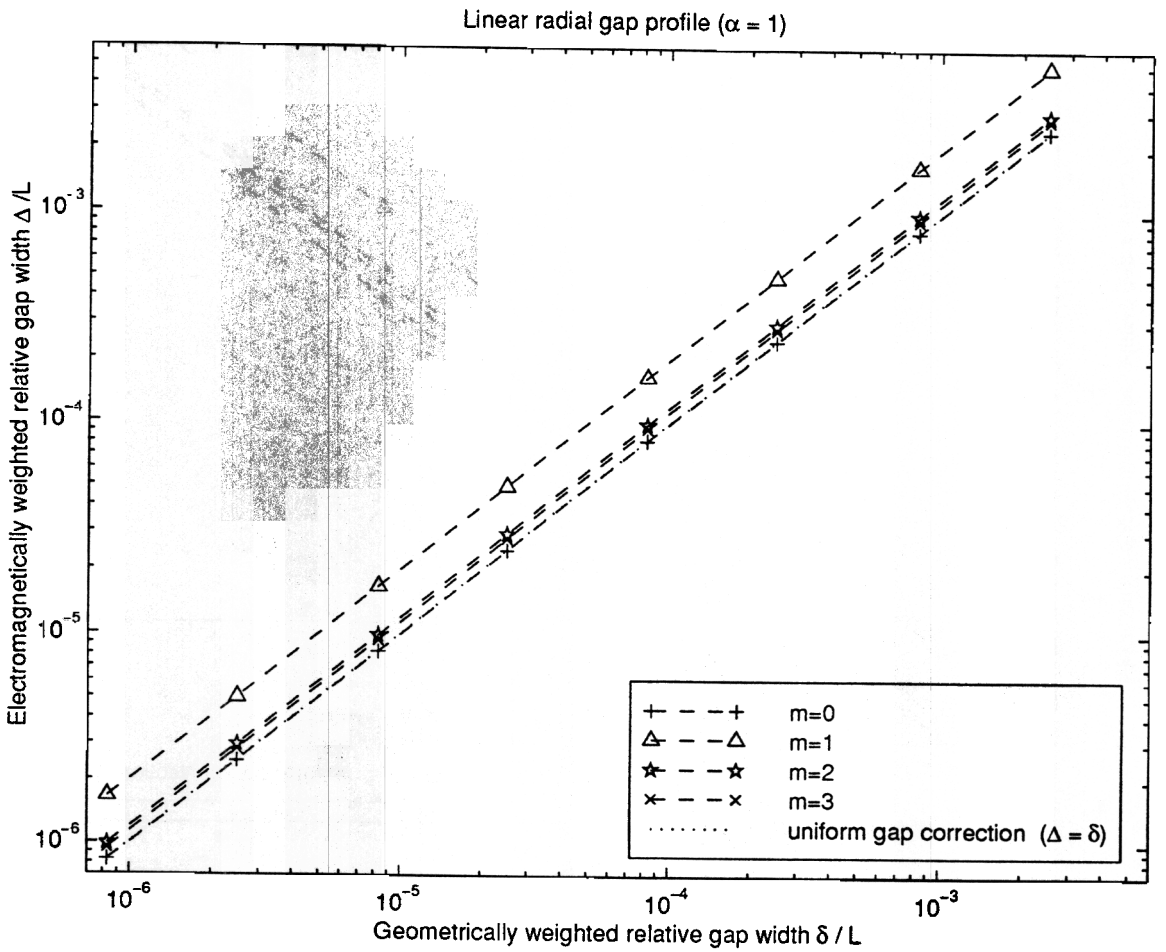

Figure 1: Gap correction for linear radial gap profile

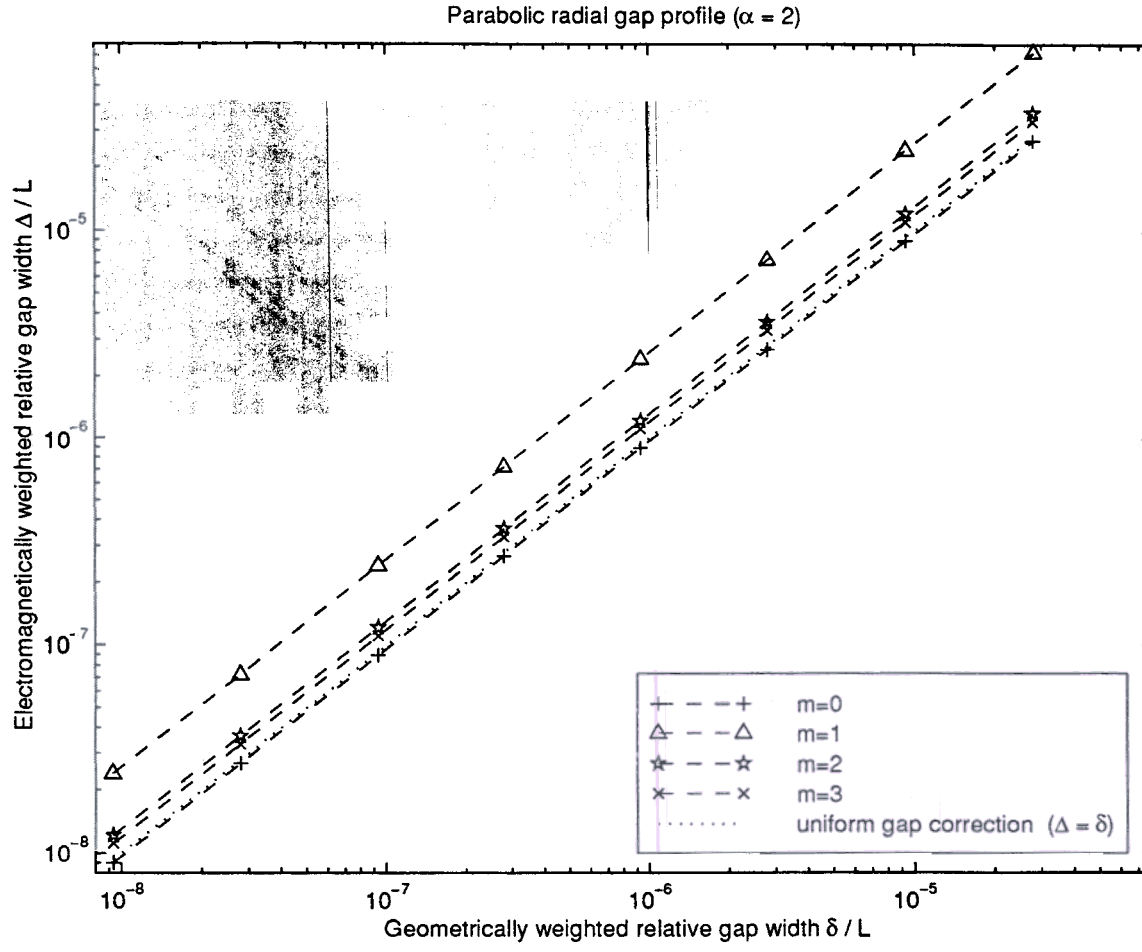

Figure 2: Gap correction for parabolic radial gap profile